



Heparosan-Coated Liposomes for Drug Delivery

DOI:

[10.1093/glycob/cwx070](https://doi.org/10.1093/glycob/cwx070)

Document Version

Accepted author manuscript

[Link to publication record in Manchester Research Explorer](#)

Citation for published version (APA):

Lane, R. S., Michael Haller, F., Chavaroche, A. A. E., Almond, A., & DeAngelis, P. L. (2017). Heparosan-Coated Liposomes for Drug Delivery. *Glycobiology*. <https://doi.org/10.1093/glycob/cwx070>

Published in:

Glycobiology

Citing this paper

Please note that where the full-text provided on Manchester Research Explorer is the Author Accepted Manuscript or Proof version this may differ from the final Published version. If citing, it is advised that you check and use the publisher's definitive version.

General rights

Copyright and moral rights for the publications made accessible in the Research Explorer are retained by the authors and/or other copyright owners and it is a condition of accessing publications that users recognise and abide by the legal requirements associated with these rights.

Takedown policy

If you believe that this document breaches copyright please refer to the University of Manchester's Takedown Procedures [<http://man.ac.uk/04Y6Bo>] or contact uml.scholarlycommunications@manchester.ac.uk providing relevant details, so we can investigate your claim.



REVISED July 30

Heparosan-Coated Liposomes for Drug Delivery

**Rachel S. Lane¹, F. Michael Haller², Anais A. E. Chavaroche², Andrew Almond³,
Paul L. DeAngelis^{*1,2}**

¹ Department of Biochemistry and Molecular Biology, University of Oklahoma Health Sciences Center, Oklahoma City, OK 73126, USA

² Caisson Biotech, LLC, 655 Research Park, Oklahoma City, OK 73104, USA

³ School of Chemistry, Manchester Institute of Biotechnology, The University of Manchester, Manchester M1 7DN, UK

* To whom correspondence should be addressed: Tel: 1-405-271-2227 x 61210;
FAX: 1-405-271-3092; email: paul-deangelis@ouhsc.edu

Key Words: cancer/chemoenzymatic synthesis/ doxorubicin/glycosaminoglycans
/polyethylene glycol

Running Title: Heparosan-Coated Liposomes

Supplementary Data Included: Supplementary Figures 1-4; Supplementary Table 1.

Abstract

Liposomal encapsulation is a useful drug delivery strategy for small molecules, especially chemotherapeutic agents such as doxorubicin. Doxil[®] is a doxorubicin-containing liposome (“dox-liposome”) that passively targets drug to tumors while reducing side effects caused by free drug permeating and poisoning healthy tissues. Polyethylene glycol (PEG) is the hydrophilic coating of Doxil[®] that protects the formulation from triggering the mononuclear phagocyte system (MPS). Evading the MPS prolongs dox-liposome circulation time thus increasing drug deposition at the tumor site. However, multiple doses of Doxil[®] sometimes activate an anti-PEG immune response that enhances liposome clearance from circulation and causes hypersensitivity, further limiting its effectiveness against disease. These side effects constrain the utility of PEG-coated liposomes in certain populations, justifying the need for investigation into alternative coatings that could improve drug delivery for better patient quality of life and outcome.

We hypothesized that heparosan (HEP; [-4-GlcA- β 1-4-GlcNAc- α 1-]_n) may serve as a PEG alternative for coating liposomes. HEP is a natural precursor to heparin biosynthesis in mammals. Also, bacteria expressing a heparosan extracellular capsule during infection escape detection and are recognized as ‘self,’ not a foreign threat. By analogy, coating drug-carrying liposomes with HEP should camouflage the delivery vehicle from the MPS, extending circulation time and potentially avoiding immune-mediated clearance. In this study, we characterize the post-modification insertion of HEP-lipids into liposomes by dynamic light scattering and coarse-grain computer modeling, test HEP-lipid immunogenicity in rats, and compare the efficacy of drug

delivered by HEP-coated liposomes to PEG-coated liposomes in a human breast cancer xenograft mouse model.

Introduction

Passive delivery of many cancer chemotherapeutics, including liposome- or nanoparticle-based systems, is accomplished by capitalizing on the dysregulated vasculature of tumors. These blood vessels exhibit a 'leaky' endothelial lining that can be extravasated by molecules normally too large to traverse healthy, non-cancerous endothelia. This phenomenon, part of the "enhanced permeability and retention effect" (EPR), passively targets drugs with ~20-200 nm diameter or ~40-200 kDa to the tumor site, while avoiding or minimizing deposition in healthy tissue (Acharya and Sahoo 2011; Grobmeyer and Moudgil 2010; Albanese et al. 2012). Many small molecule chemotherapeutics fall below this size/mass threshold and must be modified to employ EPR-based targeting. Doxorubicin with a mass of 540 Da, for example, is too small to take advantage of the EPR effect, quickly diffusing into both benign and cancerous tissue without discrimination. To extend doxorubicin's half-life, it has been encapsulated within a liposome ("dox-liposome"; commercially Myocet®), resulting in a particle size >100 nm, that helps to exclude the drug from extravasation into healthy tissue. Unfortunately, the dox-liposome's lipid bilayer membrane is susceptible to clearance by the mononuclear phagocyte system (MPS), limiting its plasma half-life to ~2.5 hours ("PEGylated Doxosome" 2014).

Another version of a cancer-fighting dox-liposome, Doxil®, is a Food & Drug Administration-approved (FDA) formulation that uses polyethylene glycol (PEG) to coat the liposomal surface, shielding the bilayer membrane from the MPS and thus extending its plasma half-life to ~55 hours ("PEGylated Doxosome" 2014). While the prolonged half-life conferred by PEGylation enables more drug to be delivered to the

tumor, it also may be responsible for a primary limitation in Doxil[®]'s use: the development of palmar-plantar erythrodysesthesia (PPE), also known as “hand-foot syndrome” (Yokomichi et al. 2013). PPE begins as a burning rash on the hands and/or feet before developing into ulcers. It is proposed that PEG-coated liposomes leak from capillaries into extremities, causing the rash to develop (Sathyamoorthy and Dhanaraju 2016). Uncoated liposomes have less occurrences of PPE, but drug tolerance (i.e. the amount of drug that can be provided to a patient without inducing side-effects) is also reduced, requiring smaller doses of drug be given, making it a less viable alternative (Waterhouse et al. 2001).

While PPE is currently thought to be the greatest dose-limiting factor for Doxil[®], another potential threat to PEG use in drug delivery systems of any form (e.g., micelles, nanoparticles, liposomes, conjugates) is the increasing prevalence of anti-PEG antibodies (Rafiyath et al. 2012). PEG is an artificial plastic that does not occur naturally in any animal and thus has the potential to promote antibody production after its initial presentation to the body. Several research groups have shown that PEGylated liposomes are subject to accelerated blood clearance (ABC) after repeated doses in mice, rats, and rhesus monkeys (Ishida and Kiwada 2008; Abu Lila et al. 2013). One group showed that a concordant increase in IgM antibody production followed the initial PEG-liposome dose (Ishida et al. 2006). This immune response reduces the circulation time of drug-loaded liposomes, potentially decreasing drug deposition at the tumor and negating the original purpose of the PEG-coating.

Although the ABC phenomenon has not yet been reported in humans, it may be a latent threat. Approximately 24% of the naïve human population (i.e. never received

an injection of a PEG-containing therapeutic) possesses anti-PEG IgM and IgG antibodies, with ~7% of the population having titers >1:80 (Lubich et al. 2016). It has been hypothesized that the production of these antibodies may be triggered by the prevalence of PEG and PEG-like molecules in everyday consumer products, such as cosmetics, laxatives, over-the-counter medications, etc (Armstrong et al. 2007). The Lubich study also found that the youngest adult population tested (18-30 years old) had the highest incidence of anti-PEG antibodies. Since the average cancer patient is over the age of 65 (National Center for Health Statistics 2016), PEG antibodies may not be a current problem, but as the younger PEG-sensitized generation ages, the necessity for a PEG alternative could increase.

In addition to antibody production, another immune response, complement activation, is elicited by free PEG infusion as well as specifically by Doxil[®] therapy (Hamad et al. 2008; Chanan-Khan et al. 2003). Complement activation is hypothesized to promote hypersensitivity reactions, or “C activation-related pseudoallergies” (CARPA), in patients receiving Doxil[®]. IgM production and complement activation are proposed to synergistically promote the ABC phenomenon; complement components complex with the IgM-tagged liposome to enhance endocytosis/clearance (Yang et al. 2013; Abu Lila et al. 2013).

Here, we present a potential natural polysaccharide alternative to the artificial PEG polymer for coating liposomes: the glycosaminoglycan (GAG) heparosan, [-4-GlcA- β 1-4-GlcNAc- α 1-]_n. In mammals, HEP is the backbone precursor of the highly sulfated heparan sulfate (HS)/heparin molecules which are essential for life. HS has many binding protein partners that spawn a plethora of interactions and signaling events

on the cell surface, in the matrix, and in the bodily fluids. The unsulfated HEP polymer, however, appears to be biologically inert in the extracellular spaces; it is not known to participate in biological binding interactions (DeAngelis 2015). This feature potentially allows certain pathogenic bacteria (e.g., *Pasteurella multocida* Type D, *Escherichia coli* K5) to invade vertebrate hosts. Microbes secrete HEP as an extracellular coating, called a capsule, employing it as molecular camouflage by mimicking 'self' molecules, and thus allowing evasion of the host defenses. The strategy of synthetically decorating or coating drugs with HEP could improve the body's acceptance of drugs, resulting in a more stable, predictable circulation time that is not subject to ABC upon repeat dosing (U.S. patent #9,687,559 and application #20150140073, 2015; DeAngelis 2015).

In addition to potentially avoiding the ABC phenomenon, we predict that HEP will also offer several other advantages. PEG is an unnatural substance that lacks a robust biological degradation pathway; the majority of the polymer is either excreted by the kidneys or accumulates in the tissues, potentially creating vacuoles (Baumann et al. 2014; Ivens et al. 2015). To avoid renal stress, reduced doses of PEGylated drugs have been recommended for patients with compromised kidney activity (Pöschel et al. 2000). In contrast, HEP is completely biocompatible and is naturally degraded in the lysosome along with other GAGs by exoglycosidases (DeAngelis 2015), thus this natural polysaccharide will neither accumulate in the body nor add stress to the body's filtration system.

Other GAGs appear to offer similar biocompatibility and already have been tested for utility in drug delivery. Especially relevant are the attempts to use hyaluronan (HA) or heparin as coatings in liposomal drug delivery models (Chen et al. 2015; Han et

al. 2016). These GAGs are used in part to help target therapeutics to cancer (e.g., HA via up-regulated CD44 receptors, or heparin to growth factor receptors), but unfortunately both of these carbohydrates have a multitude of other binding partners within the human body that increase the likelihood that drug will be delivered to healthy tissues and/or perturb various normal pathways. For example, the use of HA or heparin in drug delivery could promote off-target uptake by the HA Receptor for Endocytosis (HARE)-expressing organs, such as the liver or lymph nodes, thus killing healthy tissues as well as sequestering drug from the intended tumor site and shortening the drug's half-life in the bloodstream (Zhou et al. 2000). Furthermore, drugs delivered with a heparin coating could interfere with the coagulation pathways and lead to hemorrhaging if the dosage exceeds a certain low threshold.

Heparin and HA are also degraded by enzymes in the blood or tissues during circulation, reducing their stability and thus minimizing their potential to take advantage of the EPR effect. In contrast, heparosan has no known extracellular degradation pathway and is stable in the bloodstream (heparanase only cuts sulfated HS/heparin species), rendering it biologically inert outside of the cell, and thus more capable of passively targeting drug to the tumor site with minimal off-target effects (DeAngelis 2015).

The use of heparosan for doxorubicin delivery has been explored recently (Chen et al. 2014). In this work, some fraction of the glucuronic acid residues of the HEP chain were chemically transformed with periodate into reactive aldehydes (opening the sugar ring between C2 and C3) and then doxorubicin was reversibly attached to these aldehydes as a Schiff base. A nanoparticulate formulation (not a liposome) resulted,

but this reagent was not investigated for *in vivo* efficacy. Chemically modifying the HEP backbone, however, may reduce or destroy its “stealthy” properties, potentially triggering an immune response as well as probably impairing degradation in lysosomes via exoglycosidases.

In summary, lack of biocompatibility or multi-partner binding limits many of the hydrophilic coatings used in liposomal drug delivery. HEP could be a better alternative to unnatural polymers and bio-active GAGs, providing passive targeting that is more selective to the tumor site. To determine the utility of heparosan in liposomal drug delivery, we generated several HEP-lipid derivatives, prepared and characterized HEP-coated liposomes, conducted an immunological challenge study in rats, and compared their efficacy to the FDA-approved benchmark PEG-coated dox-liposomes in a mouse model of human breast cancer. We hypothesized that HEP could similarly coat/camouflage drug-containing liposomes, potentially proving to be a more biocompatible, but equally effective, PEG alternative.

Results

Overview of HEP-Coating Design Rationale

Our goal was to create a heparosan polysaccharide coating on the liposome's outer surface that would interact with the aqueous bloodstream environment to shield the liposome from detrimental effects in the body, including MPS clearance.

Synchronized chemoenzymatic synthesis technology allows for quasi-monodisperse (i.e. very narrow size distributions) preparations of HEP-lipid monomers with (i) a very specific sugar chain length and (ii) defined hydrophobic anchor placement. Controlling the size and the anchor stability should enable the construction of more customizable, biocompatible liposomal drug delivery vehicles.

We created hydrophobic HEP derivatives by covalently linking a single fatty acid anchor (either a palmitoyl or a dipalmitoyl tail) to the reducing terminus of a quasi-monodisperse heparosan chain (Fig 1). We hypothesized that the acyl moiety of the tail would integrate into a pre-formed liposome's lipid bilayer, analogous to post-insertional modification protocols used for PEG-lipids (Uster et al. 1996; Nag et al. 2013). We also predicted that these two different anchors would have unique stability profiles; anchoring with two acyl chains should be more stable than a single chain. We also reasoned that these amphiphilic HEP polymers would increase the coated liposome's hydrodynamic diameter in a sugar chain size-dependent manner. In addition, anchor placement at the reducing end of the HEP chain will not interfere with the lysosomal GAG degradation pathway in which two exoglycosidases (β -glucuronidase and α -N-acetylglucosaminidase) sequentially remove monosaccharides from the non-reducing end.

We tested larger polymer chains for the HEP-coatings (7-20 kDa) than the sizes employed in the PEG-coated dox-liposomes (2 kDa) because we desired to shield the liposome surface more effectively and HEP does not have the degradation issues that the artificial PEG polymer faces. Small PEG chains are more rapidly excreted than larger PEG chains (which can accumulate in tissues in an undesirable fashion); this led, in part, to the design decision to use a very small PEG molecule for the current drug, Doxil[®]. Heparosan, however, can be employed in mammalian patients even in the 100-kDa size range because this GAG is totally biocompatible and can be degraded by the natural lysosomal pathway.

Heparosan-Lipid Derivatives – Synthesis and Association with Dox-liposomes

First, we created two HEP-lipid derivatives, HEP-Palmitoyl (HEP-Palm) and HEP-DiPalmitoyl (HEP-DiPalm), by modification of HEP-NH₂ polysaccharide backbones (Fig. 1A). The HEP-NH₂ construct was built using a trisaccharide (GlcA-GlcNAc-GlcA) heparosan acceptor terminated with an ethylamine aglycone that was extended by PmHS1 heparosan synthase utilizing UDP-sugar donors. The acceptor synchronized the reaction such that all final polymer products are of very similar size and supplied the amino group functionality for later chemical coupling (Sismey-Ragatz et al. 2007). The specific molecular weight of the resulting quasi-monodisperse HEP was controlled by adjusting the molar ratio of trisaccharide HEP-NH₂ donor: UDP-sugar acceptor during polymerization by PmHS1. HEP chain sizes were ascertained by gel electrophoresis (Fig. 1B), mass spectrometry, and/or multi-angle laser light scattering (MALLS).

To create HEP-Palm, the HEP-NH₂ polysaccharide was reacted with palmitic *N*-hydroxysuccinimide ester. The HEP-DiPalm synthesis first required the conversion of HEP-NH₂ to HEP-iodoacetate (HEP-I) which was then reacted with 2*R*-1,2-didecahexanoyloxy-3-mercaptopropane (DHM) to create the target HEP-DiPalm linked by a thioether bond, which is more hydrolytically stable than the phosphoester bond. This DHM-based lipid anchor is also devoid of the phosphoglycerol structure that is thought to contribute to the induction of PEG-liposome-mediated complement activation and anaphylatoxin production (Nag et al. 2015).

Next, we tested the ability of these HEP-lipid derivatives to post-insertionally modify uncoated dox-liposomes (60:40 hydrogenated soy phosphatidylcholine/cholesterol) as monitored by various experimental methods. Dox-liposomes were incubated for one hour at room temperature with various levels (0.5-2 mole percent or “mol%,” of total lipids) of 7-, 12.5-, or 20-kDa HEP-Palm (Fig. 2). The resulting dox-liposome size was assessed using dynamic light scattering (DLS) and compared to the uncoated dox-liposome diameter. There was a clear effect of HEP-Palm mass/chain length on dox-liposome hydrodynamic size (Fig. 2A, $p < 0.0001$), confirming our prediction that liposomal size can be fine-tuned by the HEP chain length. Uncoated dox-liposomes, with an initial average diameter of 120 nm, were incrementally increased by ~17 nm, 27 nm, or 39 nm when incubated with 0.5 mol% 7-kDa, 12.5-kDa, or 20-kDa HEP-Palm, respectively. These DLS values are similar to the sizes obtained via computational predictions in coarse-grained molecular modeling simulations (Table I; details described in the next section). Agarose gel analysis also showed that the

12.5-kDa HEP-Palm sugar derivative physically associated with the liposomes in centrifugation-based separations (Supplemental Fig. 1).

To verify the contribution of the HEP polymer to the observed increase in liposomal size, we incubated HEP-coated dox-liposomes with an enzyme that cleaves either heparosan (heparinase III; specifically degrades HEP and HS) or hyaluronan (ovine testicular hyaluronidase; degrades structurally similar HA, but not heparosan; negative control). Samples incubated with the HA-degrading enzyme retained their coated size, but those incubated with HEP lyase were reduced to the initial, uncoated liposome diameter (Fig. 2B). Overall, this data substantiates that dox-liposomes can be modified or coated, with HEP-Palm.

When formulated at elevated temperatures, HEP-Palm coated dox-liposomes were smaller than those prepared at room temperature (Fig 3A, $p < 0.0001$), suggesting that heat reduces coating efficiency with this HEP-derivative. Heat increases the dox-liposome's membrane fluidity, likely allowing HEP-lipids to integrate more easily (Fan and Evans 2015). Unfortunately, the same thermal effect also augments the instability of integration, allowing the HEP-lipid to escape back into the aqueous environment. The increased temperature, however, did not induce drug leakage (as monitored by absorbance at 500 nm of the supernatant of centrifuged reaction mixtures), suggesting that the lipid membrane integrity was not damaged by heating.

For the HEP-DiPalm studies, dox-liposomes were post-insertionally modified with either 0.5 or 2 mol% of the 13.3-kDa derivative at 22°C, 37°C, or 50°C for 1 hour. At all temperatures, both concentrations of HEP-DiPalm increased the dox-liposome size, but the 2 mol% dox-liposomes were larger (Fig. 3B, $p < 0.0001$ for concentration, TwoWay

ANOVA) than those incubated with 0.5 mol% HEP-DiPalm (Fig 3B). However, formulation at 50°C with 0.5 mol% HEP-DiPalm increased dox-liposome size (+32 nm) compared to incubation at 22°C or 37°C suggesting that this HEP-lipid association or coating efficiency increases with higher temperatures.

This temperature effect on formulation efficiency was confirmed by direct radiolabeled HEP-lipid probe association measurements using size exclusion chromatography (SEC) separations. We synthesized a tritiated HEP-DiPalm probe (end-labeled with a radioactive monosaccharide) to monitor the fate of the HEP-lipid molecules. When dox-liposomes were incubated at 50°C, approximately 40% more [³H]HEP-DiPalm was found in the SEC void volume fractions (containing the liposomes) compared to those made at 37°C. HEP-DiPalm-coated dox-liposomes were reduced to their initial size after incubation with HEP lyase (Fig. 2B) in a similar fashion to the HEP-Palm experiments. Overall, these results show that the dox-liposome diameter can be modified by HEP-DiPalm and is dependent on both concentration and incubation temperatures. The additive influence of temperature on size indicates that enhanced membrane fluidity stimulates HEP-DiPalm association with the liposome and that two C-15 alkyl chains improve the coating stability in comparison to a single C-15 alkyl anchor in HEP-Palm.

Theoretical Modeling of HEP-Coated Liposomes

The exact HEP-lipid concentration in dox-liposomes could not be quantified by direct carbazole assay of the preparations due to interference from the lipid components. Computer simulations were therefore employed to investigate the

relationship between HEP chain size and loading density on the HEP-liposome hydrodynamic size, taking advantage of recent, accurate microsecond simulations of HEP oligosaccharides and coarse-graining developments (Sattelle et al. 2013). Simulations were conducted from 0.1 mol% to 0.5 mol% (the input concentration) HEP-DiPalm to represent the potential concentration range of coating-derivative associated with the liposome. Briefly, coarse-grained representations of 13.3-kDa HEP polymers were anchored onto a spherical boundary at four concentrations and simulated for 1.5 nanosec (ns) to allow the assembly to equilibrate, which was observed to occur within 0.5 ns in all cases (Supplemental Fig. 2). Molecular configurations were output every picosec and used to predict hydrodynamic volume (V_h) as a function of simulated time. The average value of the hydrodynamic radius ($r_h = \left(\frac{3V_h}{4\pi}\right)^{1/3}$) over the final 1 ns was used to provide an experimental prediction. Comparison with the DLS-derived diameter for 13.3-kDa HEP-DiPalm (149 nm) indicated that the loading concentration was predicted to be in the range 0.4-0.5 mol%. Further simulations were conducted with HEP sizes in the range 7-kDa to 20-kDa at 0.5 mol% and these were also compared with DLS experiments (Table I). As expected, reduction in both HEP-lipid density and chain size during modeling resulted in lower r_h . The predicted values for r_h for HEP-liposome systems were in good agreement with DLS, especially in the 7 to 13.3 kDa range, giving some confidence that our extensive simulations provided insight into the microscopic state of the HEP-liposome assembly. Typical images from HEP-liposome simulations with 7-kDa and 13.3-kDa HEP are depicted in Fig. 4.

Even without knowing the exact HEP amount on the liposomes, we obtained substantial HEP-coatings based on the DLS data showing a plateau in the maximal

hydrodynamic size following HEP-lipid titrations (Figs. 2, 3 and data not shown), indicating that surface saturation was achieved. This interpretation was confirmed by simulations of 13.3-kDa HEP-DiPalm at increments between 0.1-0.5 mol% (Supplemental Fig. 2). Theoretical prediction of coating with 0.4 mol% versus 0.5 mol% HEP-DiPalm showed little effect on hydrodynamic radius.

In model sphere penetration simulations (Supplemental Fig. 3), it is predicted that the movement of larger macromolecules ($r_h > 15$ nm; e.g., the megaDalton complement complex) through the saturated (0.4-0.5 mol%) HEP coating to the liposome bilayer surface may be prevented while smaller proteins (IgM, 12.7 nm; IgG, 5.4 nm; Armstrong et al. 2004) would be partially excluded. Preliminary studies using bacterial pore-forming toxins (which act in a mechanism akin to the complement system) in a dye-loaded liposome model (Hotze et al. 2013) suggested that the HEP-coating could prevent lysis (data not shown). Thus, macromolecules in the bloodstream should also be hindered from interacting with the lipid bilayer, a goal of this study.

Stability of HEP-Coated liposomes

The HEP-DiPalm association or incorporation with the dox-liposome was determined to be stable under various challenges. A tritiated HEP-DiPalm probe was incubated with dox-liposomes under the optimal conditions (0.5 mol% input, 50°C for 1 hour as determined by DLS), then any free unincorporated HEP-DiPalm was removed from the dox-liposome-associated HEP by size exclusion chromatography (SEC). These purified radiolabeled HEP-coated dox-liposomes were then challenged by incubation either in human plasma or in PBS at 37°C for a day, then the samples were

re-analyzed by SEC. The PBS-treated samples retained ~92% of the radioactive probe in the liposomal fraction, while plasma-challenged samples retained ~80% (Fig. 5). This comparison suggests that, while the plasma does partially compromise the HEP-DiPalm coating, the majority of the HEP-DiPalm is stably integrated into or associated with the dox-liposome.

We also attempted to measure the stability of HEP-Palm using this radioactive probe method. Unfortunately, due to poor overall recovery of this monoacyl radiolabeled probe in the SEC eluate (perhaps due to interaction of the column resin with the free acyl tail), we were unable to quantitatively assess the stability.

HEP-Dox-liposome Efficacy Evaluation

To test HEP-dox-liposome efficacy against cancerous tumor growth, we conducted *in vivo* studies using the human breast cancer cell-line MDA-MB-231 implanted into immunodeficient mice, a xenograft model used in the past with dox-liposomes (Anders et al. 2013; Mamidi et al. 2010). Cells were orthotopically placed into the cleared, right mammary gland of female NRG mice (NOD.Cg-Rag1tm1Mom ||2rgtm1Wjil/SzJ). This mouse strain was chosen because it exhibits reduced weight loss with doxorubicin treatment (personal communication, Dr. Magdalena Bieniasz). Mice were treated with (i) saline vehicle, (ii) undecorated dox-liposomes, (iii) 5 mol% PEG-coated dox-liposomes (2-kDa PEG; "Doxil[®]"), and dox-liposomes decorated with 0.5 mol% of either (iv) HEP-Palm (12.5-kDa) or (v) HEP-DiPalm (13.3-kDa). Drug coating by HEP-Palm and HEP-DiPalm was qualified by DLS for each batch used in dosing. This batch of uncoated dox-liposomes, destined for the efficacy study, was

manufactured separately from those used for characterization studies and had a slightly larger initial uncoated diameter (129 nm). However, the addition of HEP-lipid resulted in roughly equivalent relative r_h increase (+29 nm or +30 nm for 12.5-kDa HEP-Palm or 13.3-kDa HEP DiPalm, respectively; Fig. 6) as the formulation in earlier characterization studies (noted in Table I and Fig. 3).

Tumor growth was significantly reduced compared to the PBS vehicle control in all treatment groups; in fact, in this aggressive cancer model, all un-medicated control animals died or were sacrificed for humane reasons (i.e. tumor rupture of skin) prior to study completion. PEGylated or HEP-DiPalm dox-liposomes significantly reduced tumor volume and mass compared to the uncoated dox-liposomes or the HEP-Palm dox-liposomes (TwoWay ANOVA, ** $p < 0.01$, * $p < 0.05$, respectively, Fig. 7A; ** $p < 0.01$, Fig. 7B). This data implies that the more stable DiPalm anchor confers greater efficacy than the HEP-Palm. Interestingly, while the outcome of the two treatments with PEG or HEP-DiPalm-coated formulations were not significantly different from each other, suggesting similar efficacy, the histopathological assessment revealed a significant incidence of necrosis in tumors treated with HEP-DiPalm compared to all other treatment groups, suggesting the potential for enhanced potency or efficacy (OneWay ANOVA, ** $p < 0.01$, Fig. 7C).

As chemotherapeutics often have detrimental side effects, the blood and organs of the mice were analyzed for signs of disease and toxicity (Supplemental Table I). Blood chemistries were compared to established normal limits for rodents (Rosenthal 2002). Alkaline phosphatase (ALP) was elevated in PEG dox-liposome-treated mice compared to the HEP-DiPalm, but there were no discriminating histopathological signs

of liver disease. Another source of elevated ALP is bone damage, but, since this finding was unexpected prior to tissue sampling, bone was not available for further examination post-mortem. Hearts and spleens did not display any signs of toxicity or disease. Both PEG- and HEP-DiPalm dox-liposomes reduced lung metastasis compared to uncoated dox-liposomes, but HEP-DiPalm was not quite as effective as PEG in this regard (Supplemental Table I).

Interestingly, the HEP-Palm and -DiPalm treatment groups had significantly better blood and urea nitrogen (BUN) levels compared to PEG-coated dox-liposomes ($p < 0.05$, $p < 0.005$, respectively, Supplemental Table I), but there was no histopathological evidence to support renal failure. This observation advocates that heparosan, a biocompatible molecule in mammals, could potentially reduce the renal load. Previous studies have suggested lower doses of PEGylated drugs may be prudent in patients with kidney dysfunction (Pöschel et al. 2000). HEP-DiPalm mediated drug delivery could provide a full chemotherapeutic dose to kidney-compromised patients.

Immunogenicity Testing of HEP-DiPalm Derivative in Rats.

To further evaluate safety, a long-term immunological study of three HEP-conjugated molecules was performed in rats (**Supplementary Fig. 4**). In brief, a trio of serial tandem challenges with HEP-granulocyte colony stimulating factor (G-CSF) (Jing et al. 2017, submitted), HEP-phenylalanine ammonium lyase, and HEP-DiPalm were performed. While antibodies against human G-CSF started to appear as early as in the first post-injection bleed (the rat and the human proteins are non-identical at the amino acid sequence level and the attachment of a single HEP chain is not expected to

completely shield the drug surface; *data not shown*), no IgM or IgG antibody directed against heparosan was detected even after multiple injections including three boosts of HEP-DiPalm over the 63-week study span (**Fig. 8**). The wells with BSA alone, the negative control for assessing assay background, had comparable signals to wells with HEP-BSA conjugate or HEP-DiPalm.

Discussion

PEG is a foreign substance that, in some cases, can signal a threat to the body, activating the immune system to attack or clear the invader. In contrast, heparosan is a natural component in mammals making it an unlikely antigen or immune trigger. We have characterized a simple post-insertional modification method for the addition of HEP-lipids to dox-liposomes. In addition, we have demonstrated that HEP-lipid coated dox-liposomes were as potent as FDA-approved PEG-based formulations in reducing tumor growth in this human xenograft model and may have other desirable attributes.

PEG's artificial nature not only makes it a target for clearance by the immune system, but also potentially increases the burden on detoxification organs, such as the liver and kidneys, since the plastic does not have a biological degradation pathway aside from simple filtration and excretion (Ivens et al. 2015). HEP is biocompatible, an advantage conferred by its natural biosynthesis and metabolism in all animals. Although there were no histopathological signs of renal toxicity, PEG-treated animals did exhibit increased nitrogen levels in the blood and urea tests, suggesting that renal function was perhaps compromised. HEP-DiPalm-treated animals had a normal range of nitrogen levels and thus may be a better alternative for both healthy patients and those with reduced renal function. In addition, no sign of an immune response against heparosan was noted after multiple injections of HEP-biologic drugs and HEP-lipid thus such HEP-coated nanoparticles should be useful over a long courses of treatment and/or when pre-existing high anti-PEG titers in some patients precludes the use of the original PEGylated drug.

In this work, we tested the hypothesis that HEP-lipids can integrate into liposomes, serving as an equally efficacious drug delivery model to PEGylated dox-liposomes. As predicted, HEP anchored with a single palmitoyl group was not as stable as when the sugar polymer was attached to a dipalmitoyl group, and therefore future studies will probably benefit from focusing on the use of more hydrophobic derivatives such as HEP-DiPalm.

Predictive large-scale computer simulations, as demonstrated here, can be used to dissect physical properties of HEP-coated liposomes and hence provide insights into their potential biological behavior. Combined with the highly controllable chemoenzymatic synthesis of targeted sugar chain sizes, molecular simulations *in silico* may be useful to accelerate the design of next-generation HEP-coated liposomes with defined hydrodynamic, molecular exclusion, or multivalent interactional behavior thus saving time and cost of syntheses as well as reducing the extent of animal testing.

Our computer simulations were fairly accurate in predicting the effect of smaller (<14 kDa) HEP-DiPalm chains on the hydrodynamic diameter, based on their agreement with the DLS data. The modeling, however, potentially over-estimated the contribution of larger HEP-lipids (20 kDa) on liposome size. This discrepancy with larger HEP chains could be due to assumptions built into the model, such as the validity of using the Debye-Hückel theory of ionic solutions in this assembly or the method used for estimating hydrodynamic volume. Perhaps longer HEP monomer chains shroud the diacyl group, impeding association with the liposome. Alternatively, and perhaps more likely based on the sphere penetration modeling, when approaching saturation these longer, integrated HEP chains sterically hinder or shield the liposome bilayer surface

from further incorporation of additional HEP-DiPalm monomers. While computer simulations may represent the potential of a HEP-lipid for modifying liposome size, experimental testing and/or further modeling parameter optimization may be required to actually achieve that ideal in the larger sugar chain size regime. Simulations may also provide insight into the mechanics of HEP-lipid liposome association in solution.

HEP-DiPalm dox-liposomes impaired tumor growth in a mouse cancer model similar to FDA-approved PEG-coated dox-liposomes, and also exhibited potentially unique properties that need to be further characterized. Other existing drugs that have been delivered in liposomal formulations may also benefit from the HEP-coating technology platform. Additional benefits of using this HEP-coating system include: (i) post-insertional modification is a quick method to coat an established liposomal formulation *in situ*, thus simplifying the manufacture process, (ii) improvement of a well-known drug that has already been tested in clinical trials should reduce regulatory risks and costs, and (iii) this new intellectual property allows drug life-cycle management conferring extended patent life.

Materials and Methods

Reagents and Cells

The HEP polymer was synthesized by recombinant *Escherichia coli*-derived *Pasteurella multocida* heparosan synthase 1 (PmHS1), fused to a maltose-binding protein, cloned and purified using a previously established method (Sismey-Ragatz et al. 2007). Sterile suspensions of dox-liposomes, liposomes composed of 60 mol% hydrosoyphosphatidylcholine (HSPC) and 40 mol% cholesterol, loaded with doxorubicin (16 mg/mL lipids; 2 mg/mL drug), were purchased from Encapsula Nanosciences (Brentwood, TN) in either an uncoated form or formulated with 5 mol% 2-kDa polyethylene glycol-distearoyl phosphoethanolamine (PEG-DSPE). UDP-[³H]GlcA and UDP-[³H]GlcNAc were from Perkin Elmer (Waltham, MA). The MDA-MB-231 human breast cancer cell line was obtained from ATCC (# 62657852; Manassas, VA) and verified to be free of Hantaan virus, LCMV, and *Mycoplasma sp.* by external validation via polymerase chain reaction (Mamidi et al. 2010). Sterile, endotoxin-free water was used to prepare buffers used in HEP-lipid syntheses. All other reagents were purchased from Sigma-Aldrich (St. Louis, MO) in the highest quality possible unless otherwise indicated.

HEP-Palmitoyl Synthesis

The HEP polysaccharide with a palmitoyl anchor was made in a two-step process. First, various sizes of heparosan chains with a free amine at the reducing terminus (HEP-NH₂) were prepared by synchronized, stoichiometrically controlled polymerization (Sismey-Ragatz et al. 2007). A heparosan trisaccharide (GlcA-GlcNAc-

GlcA) with an ethylamine aglycone was used as the acceptor in PmHS1-mediated reactions with UDP-GlcA and UDP-GlcNAc donors (Jing et al., submitted 2017). The ratio of acceptor to donor controls the size of the final polymer chain. After overnight reaction, the target HEP-NH₂ was purified by strong anion exchange chromatography (SAX), with Sepharose Q (GE) column using 10 mM sodium acetate buffer, pH 5.8, with salt elution. The sample was applied to the column and then washed with buffer containing either 0.1 M NaCl (for 7-13 kDa polymers) or 0.15 M NaCl (for 20-kDa polymer) until the baseline at 215 nm was stable. The target polymer was eluted with a linear gradient from the wash buffer to 1 M NaCl buffer in ~30-40 min. The HEP polymers were typically eluted between 0.2-0.4 M NaCl (smaller polymers require less NaCl for elution). The HEP peak (absorbance at 215 nm due to carbonyl groups of the amide and the carboxyl groups) was then harvested by ethanol precipitation (EtOH; 2.5 volumes) and centrifugation (4,000 x g, 30 minutes). Bulk EtOH was removed by aspiration and the pellet was vacuum-dried. Heparosan was quantified by the carbazole assay using GlcA as a standard (Bitter and Muir 1962). The polymer size was determined by SEC-MALLS (Baggenstoss and Weigel 2006) and/or liquid chromatography coupled with electrospray ionization mass spectroscopy (LC/MS) (Li et al. 2012). The polydispersity values were in the range of ~1.005-1.01 (for reference, "1" is an ideal polymer).

Second, palmitic *N*-hydroxysuccinimide ester (Palm-NHS; Sigma) was coupled to the HEP-NH₂. The polymer was initially dissolved in 0.1 M sodium phosphate, pH 7.0, then dimethyl sulfoxide (DMSO) was added to 80% final concentration to yield a 10 mg/mL carbohydrate solution. Palm-NHS dissolved in DMSO (10 mg/mL; 400 molar

equivalents) was then added to the HEP-NH₂ solution with mixing. The reaction was continued overnight with mixing at room temperature in the dark. The target HEP-Palm was precipitated from the reaction mixture by the addition of EtOH and NaCl to 75% and 0.1 M final, respectively, and incubation on ice for 1 hr. The precipitate was harvested by centrifugation as above, vacuum-dried, and then dissolved in water. Next, the slightly cloudy solution was filtered through 0.45 µm syringe filter and SAX chromatography was performed as described for HEP-NH₂. The target HEP-Palm in the 0.1-0.5 M NaCl fractions was harvested by EtOH precipitation as described before. Typical yields were ~80% based on sugar. Agarose gel electrophoresis analysis (2%, 1X TAE with Stains-All detection; (Lee & Cowman 1994) detected the HEP-Palm as a new species that migrated more slowly and broadly than the parent HEP-NH₂ polymer. On 8% PAGE in 1X TBE, the migration differences between the HEP parent and its lipid derivative were not readily discernible.

HEP-DiPalmitoyl Synthesis

In this synthesis, a thiol-containing lipid anchor with two palmitoyl groups was reacted with HEP-iodoacetyl (HEP-I) derivative. To create the required hydrophobic anchor, a variation of the published method (Liu et al. 2007) was employed to prepare 2*R*-1,2-didecahexanoyloxy-3-mercaptopropane (DHM). Basically, a palmitic (C16) reagent was substituted for the original hexanoyl (C6) reagent. To create the needed thiol-reactive heparosan derivatives, the HEP-NH₂ was first dissolved in 100 mM HEPES, pH 7.2, 5 mM EDTA, 42% DMSO (final concentrations; the latter solvent was added after the aqueous buffer components), then 33-54 equivalents of *N*-succinimidyl

iodoacetate (SIA; Pierce Thermo Scientific) in DMSO (1/10 volume of the reaction) was added and mixed overnight at room temperature in a foil-wrapped tube. The HEP-I polymer was recovered by isopropanol precipitation (4.8 volumes, 0.1M NaCl final; similar to EtOH method for HEP-Palm), followed by SAX on Sepharose Q resin.

Next, the HEP-I was dissolved in 33 mM sodium borate, pH 8.5, and then DMSO was added slowly until the solvent reached a final concentration of 59%. DHM (52 equivalents) in chloroform (33% final volume) was then added gradually and the reaction mixed at room temperature overnight in the dark. To enhance phase separation, more chloroform (0.25 volume) was added, vigorously mixed, then centrifuged (3,000 x g for 5 minutes) in a glass centrifuge tube. The target in the aqueous phase was collected, and two more cycles of chloroform addition (0.25 volumes each) and centrifugation drove more aqueous phase from the reaction mixture. The HEP-DiPalm polymer in the pooled aqueous phase fractions was harvested by isopropanol precipitation. A 70% isopropanol, 0.1 M NaCl wash of the pellet was performed before vacuum-drying the product.

SAX was used as before to separate the HEP-DiPalm from the unreacted HEP-NH₂ in the crude pellet, but this step did not completely resolve the two populations. Therefore, the SAX fractions containing HEP-DiPalm were subjected to ultrafiltration to separate the micellar HEP-DiPalm aggregates (which yields large MW complexes) from any remaining HEP-NH₂ monomers. The SAX fractions were concentrated in an Amicon Ultracell unit with a 15-kDa MWCO (PES filter; Millipore, Billerica, MA). The retentate, with target HEP-DiPalm, was washed thrice in 200 mM NaCl. Agarose gel electrophoresis revealed that the free HEP-NH₂ was successfully removed. Finally, the

retentate was harvested by ethanol precipitation (70% final), centrifuged, and vacuum-dried.

HEP-Lipid Characterization by PAGE

HEP-lipids were analyzed by polyacrylamide gel electrophoresis (PAGE) with 1X TBE buffer. An 8% (29:1 crosslinker) polyacrylamide gel was loaded with two $\mu\text{g}/\text{lane}$ of 7-, 12.5-, 13.3-, or 20-kDa HEP-NH₂ or HEP-lipid. The gel was run at 250 volts for 25 min and then stained with Alcian Blue as previously described (Ikegami-Kawai and Takahashi 2002).

HEP-Lipid Association Assessment by Agarose Gel

For HEP-Palm association by electrophoretic analysis, 64 μg of dox-liposomes were incubated with 0.5 or 1.0 mol% 12.5 kDa HEP-Palm in PBS (5.8 μL reaction volume) for two hours at either room temperature or 37°C. Controls included either the HEP-Palm or dox-liposome component alone that were incubated at 37°C. Samples were diluted to 400 μL and centrifuged at 20,800 $\times g$ for 60 minutes. The pellet (with liposomes) was re-suspended in 10 μL PBS and 5 μL was loaded on a 2% agarose gel, which was run at 30 V for ten minutes and then 80 V for one hour. Afterwards, the gel was stained with Stains-All for GAG detection (Lee & Cowman 1994).

HEP-Lipid Association Assessment by Dynamic Light Scattering (DLS)

For DLS size analysis of HEP-lipid coating, dox-liposomes (~50 nMoles lipids; 16 mg/mL lipids) were incubated with 0.5-2 mol% 12.5-kDa HEP-Palm or 13.3-kDa HEP-

DiPalm (based on lipids; 10 μ L reaction volume) at the specified time (1-3 hrs) and temperature (22°C-50°C). The sample was then diluted in 1 mL PBS and placed in a disposable two-sided polystyrene cuvette for size measurement in a 90Plus/Bi-MAS (532 nm laser model; Brookhaven Instruments; Holtsville, NY) at 25°C. Uncoated dox-liposomes were also measured externally at the production facility (Encapsula Nanosciences). Each sample was measured for 2 min, in triplicate. Portions of the HEP-coated dox-liposomes (1 or 2 mol%) were treated with *E. coli*-derived recombinant heparinase III (gift of the laboratory of Robert J. Linhardt, Rensselaer Polytechnic Institute; Troy, NY) or ovine testicular hyaluronidase (Sigma Type IV) overnight in 50 mM HEPES, pH 7.2, to test if the size increase was due to HEP association.

Drug Leakage Analysis

The potential leakage of drug from dox-liposomes was evaluated using samples heated at various temperatures followed by centrifugation and spectrometry of the supernatant fraction. Each sample contained 80 μ g of dox-liposomes (1.25 μ L of stock; 10 μ g doxorubicin) mixed with PBS (final volume 200 μ L) that was incubated at 0°, 37°, 50° or 65°C. After one hour, the samples were centrifuged at 20,800 x *g* for 30 min (using 'soft stop' mode) to remove the dox-liposomes from the bulk liquid. The supernatant and pellet were separately collected and diluted to a final volume of 2 mL with PBS for optical density analysis at 500 nm.

Stability of HEP-Lipid Association

The stability of HEP-DiPalm coated dox-liposomes in plasma was tested using dox-liposomes coated with tritiated HEP-DiPalm. To create the radioactive probe, HEP-DiPalm (13.3-kDa; 0.74 nMoles) was extended with 200 pmoles UDP-[³H]GlcA and 55 pmoles UDP-[³H]GlcNAc in reaction buffer with 50 mM HEPES, 2 mM MnCl₂ and 85 µg PmHS1 for 30 min; on average, this labeling adds one sugar to ~30% of the pre-existing sugar chains, thus resulting in a negligible difference in the overall chain size of the derivative. Free UDP-sugar was removed from the reaction using ultrafiltration (3-kDa MWCO Ultracon), with five sequential dilution (0.5 mL PBS each) and spin concentration steps. A portion of the resulting product in the retentate was mixed with scintillation fluid and counted to assess its specific activity.

The tritiated HEP-DiPalm (~50,000 dpm/sample; 0.5 mol% final with unlabeled reagent) was incubated with dox-liposomes (16 µg) for one hour at 50°C. To separate unincorporated HEP-lipid monomer and aggregates from dox-liposomes, the reaction was applied to a Sepharose 2B column (17 cm x 1.5 cm; 13 mL; GE Lifesciences, Marlborough, MA) eluted in PBS (fractions 0.54 mL each) that can separate liposomes from micellar assemblies. Void volume fractions (#6-9) with the dox-liposome-associated probe were concentrated using ultrafiltration (3 kDa MWCO) for use as a test article for later challenges.

These purified radioactive dox-liposomes were incubated in a 200 µl final volume with either PBS or pooled normal human plasma (freshly thawed cryogenic stock; PrecisionBioLogic CryoCheck; Dartmouth, Nova Scotia, Canada) at 37°C for 24 hrs. The two challenged samples were again applied to the Sepharose 2B column and the

void volume was collected and counted for dox-liposome-associated radioactivity (A_c). These values were compared to the signal from the initial, unchallenged sample (A_i) that identically processed by SEC. Stability (A_s) was assessed as $\frac{A_c}{A_i} \times 100 = A_s$.

Molecular Simulations of Heparosan-Coatings on Liposomes

Simulations were performed using the SimTK molecular modeling API adapted for carbohydrates (Sherman et al. 2011) run on an Intel i7-4770K microprocessor (Santa Clara, CA). Rings were maintained in 4C_1 -chair conformation and polymers constructed such that glycosidic angles were modeled as pin joints, with torques applied according to a coarse-grained potential defined previously for heparosan (Sattelle et al. 2013). The reducing termini of extended heparosan polymers (with a quantity according to mol% of lipid) were uniformly welded to the surface of a 59-nm radius sphere, which was modeled as a hard solid. The number of monosaccharide units (derived from GlcA-GlcNAc repeat averaged to ~189.5 Da/sugar) per HEP chain used was 37, 66, 70, or 106 for the 7, 12.5, 13.3, or 20 kDa polymers, respectively. A single negative charge was situated on every disaccharide (corresponding to the GlcA residue's carboxylate moiety) and repulsion simulated using a Debye-Hückel interaction potential with a fully dissociated ionic strength of 150 mM (i.e. physiological conditions) (Bathe et al. 2005). The assembly was heated to 20°C by velocity rescaling and free dynamics calculations performed using the Verlet integration algorithm for 1.5 ns for the following seven setups: 20-kDa at 0.5 mol%; 13.3-kDa at 0.1, 0.2, 0.4 and 0.5 mol%; 12.5 k-Da at 0.5 mol%; 7-kDa at 0.5 mol%. Hydrodynamic volume (Supplemental Fig. 2) was calculated using Monte-Carlo sampling in a 200 nm cube using a 10 nm radius test sphere, based

on an approach described previously (Ortega et al. 2011), and estimated from time series following a period of equilibration.

An equivalent method was used to calculate the penetration depth of various exteriorly located macromolecules found in plasma. In this case, the test sphere radius was varied between 2 and 60 nm and Monte-Carlo sampling was used to identify the closest distance of approach to the lipid surface at which it did not clash any HEP chain from a typical equilibrated molecular configuration extracted from the simulation (Supplemental Fig. 3).

Efficacy Testing of HEP-Dox-liposomes in Tumor Model

NOD.Cg-Rag1^{tm1Mom} Il2r^{gtm1Wjl}/SzJ (NRG) mice were purchased from Jackson Laboratories (Harbor, ME) for use as the recipient in a human breast cancer xenograft model. This study was approved by the Oklahoma Medical Research Foundation IACUC on September 18, 2014. For tumor placement, the inguinal #4 mammary gland was first removed, enabling orthotopic implantation of the doxorubicin-sensitive, human breast cancer cell line, MDA-MB-231. Cells were suspended in 70% PBS/30% Matrigel (Cat. #47743-720; Corning Life Sciences; Corning, NY) and 3×10^6 cells were injected per site. Once the tumors reached an average size of $\sim 100 \text{ mm}^3$, mice were randomized into groups of nine, and treatment groups received three doses of the various liposome-encapsulated doxorubicin formulations (6 mg/kg) or the PBS vehicle. Doxorubicin was provided in either: A) uncoated, drug-filled liposomes (“dox-liposomes”); B) dox-liposomes prepared with 5 mol% polyethylene glycol-distearoyl phosphoethanolamine (PEG-DSPE, 2-kDa PEG; Encapsula Nanosciences) (generic

comparable to “Doxil[®]”); C) dox-liposomes coated with 0.5 mol% 12.5-kDa HEP-Palm; or D) dox-liposomes coated with 0.5 mol% 13.3-kDa HEP-DiPalm. The formulation of dox-liposomes was done on the day the dose was given; liposomes were either incubated with HEP-Palm (1 hour at room temperature) or with HEP-DiPalm (1 hour at 50°C) in closed tubes under a nitrogen gas blanket. Doses #1, #2, and #3 were given on Day 1, 10, and 20, respectively.

Tumor volume was measured every 5 days by a TumorImager (Biopticon Corporation; Princeton, NJ), an image acquisition and processing system that uses laser-scanning measurements to calculate more precise tumor volumes through algorithms. Mice were sacrificed 14 days after the third and final dose. Blood, tumor, and relevant organs (heart, liver, tumor, spleen, kidneys, lungs) were collected for further analysis. Blood chemistry (ALT, ALP, and BUN) was analyzed by Antech Diagnostics (Stillwater, OK).

Histopathology

Histopathology was conducted by a board-certified veterinary pathologist at the University of Oklahoma Health Sciences Center. At harvest, organs were placed into 10% neutral buffered formalin for a minimum of 48 hrs before being embedded in paraffin blocks for sectioning. Blocks were sectioned (5 µm), affixed to glass slides, and stained with hematoxylin and eosin. Thirty high power fields of view were examined per specimen; the entire process was performed in duplicate on separate days by the same pathologist and the two values were averaged.

Immunological Challenge Study in Rats

To verify the predictions that heparosan, a 'self' molecule, would not be immunogenic, the HEP-DiPalm micellar preparation was tested in a rat model; in this study, the animals had previously been with two different HEP-protein conjugates (Jing *et al.* 2017; submitted) before boosting 3 times with the HEP-coating reagent (**Supplementary Figure 4**). Basically, three male Sprague-Dawley rats were injected subcutaneously in the dorsal region with HEP-granulocyte colony stimulating factor (G-CSF) in saline every three weeks at a level of 0.4-0.7 mg/kg (9 injections over 7 months) in an IACUC-approved protocol (SDIX, LLC; Newark, DE). Then a HEP-phenylalanine ammonium lyase (a microbial enzyme for treating phenylketonuria) conjugate was injected with three doses (0.2-0.4 mgs protein in saline every 3 weeks). Finally, the rats were injected with HEP-DiPalm in saline (0.4 mg/dose) every 3 weeks; as noted in Fig. 1B (see lane 6), this derivative forms micelles in aqueous buffers when present above the critical micellar concentration (~10 μ M in neutral saline via the pyrene fluorescence method; Aguiar *et al.* 2003).

Blood for production of serum were collected after the HEP-PAL injections (Week 48) and for this study, 2 weeks after the last HEP-DiPalm boost (**Supplementary Fig. 4**; *note*: Week 1 and 48 bleeds had equivalent background responses to HEP-BSA or BSA wells so both sera were used in the various assays). The bleeds were frozen and shipped backed to Caisson Biotech, LLC in Oklahoma City, Oklahoma for testing for the potential presence of anti-HEP-antibodies by ELISA with goat anti-rat IgG or IgM as the secondary antibodies (horseradish peroxidase conjugates; Thermo Scientific). All steps were performed at room temperature.

Amine-binding maleic anhydride plates (Thermo Scientific) were coated with 200 μ L of antigen solution (55-kDa heparosan-amine at 0.1 mg/mL). Other wells were coated with 100 mM Tris, pH 7.2 or bovine serum albumin (BSA; Promega) as negative controls, or 0.1 mg/mL HEP-BSA (a heparosan conjugate produced via reductive amination in analogy to HEP-G-CSF). The immobilization of HEP-BSA to the well surface was verified and validated by radiochemical tests of tritiated UDP-sugar incorporation mediated by the heparosan synthase, PmHS1. Likewise, the HEP-DiPalm reagent (2 μ g/well) was verified to be immobilized; in this case, the plastic surface of the well was sufficient for binding the lipid. In all cases, at least triplicate wells were tested for each antigen above.

After 4-6 hours incubation with the various test antigens at room temperature, the plates were washed with PBST and blocked for overnight with 1% in PBST (phosphate buffered saline with 0.05% Tween). The test sera (0.5-5 μ l/well) diluted in PBST with 1% BSA were added to the wells for 2-3 hours of incubation. After thoroughly washing wells with PBST, horseradish peroxidase-conjugated goat polyclonal anti-rat IgG or IgM (Thermo Scientific) detection agents diluted in PBST with 1% BSA were added to the wells and the plates were incubated for 2 hrs. After final washing with PBST, a peroxidase substrate solution (TMB Substrate Kit, Thermo Scientific) for color development was added. The reaction was stopped after 30 min with 2M H_2SO_4 and the intensity of the color was measured by a spectrophotometric plate reader at 450 nm. The data from triplicate wells was averaged and shown with standard deviation. The ELISA tests were repeated as 2-3 independent assays on different days.

Abbreviations: ABC, accelerated blood clearance; DHM, 2R-1,2-didecahexanoyloxy-3-mercaptopropane; DLS, dynamic light scattering; DMSO, dimethyl sulfoxide; EPR, enhanced permeability and retention effect; EtOH, ethanol; FDA, Food and Drug Administration; GAG, glycosaminoglycans; HA, hyaluronan; HEP, heparosan; HEP-DiPalm, heparosan-dipalmitoyl; HEP Lyase, Heparinase III; HEP-Palm, heparosan-palmitoyl; MPS, mononuclear phagocyte system; PBS, phosphate buffered saline; PmHS, *P. multocida* HEP synthase; PPE, palmar plantar erythrodysesthesia; PEG, polyethylene glycol.

Acknowledgements: We thank: Dixy E. Green for general laboratory support, and manuscript review; Dr. Robert Linhardt for the gift of HEP lyase and the mass spectrometry work. Dr. Stanley Kosanke for expert advice on histopathological interpretations; Dr. Magdalena Bieniasz for cancer animal model design and insight; Lin Wang for animal supervision; Dr. Vibhu Awasthi for assistance interpreting lipid behavior; Dr. Ann L. Olson for guidance on blood chemistry and statistical analyses; and Drs. Rod Tweten and Eileen Hotze for providing liposome preparations for the pilot tests. We recognize funding by the Oklahoma Center for Advancement of Science and Technology (OCAST) and National Institutes of Health SBIR grant (1R43CA159494-01) to PLD for support of some pilot stages of work.

Conflict of Interest Statement: Drs. Chavarroche, DeAngelis & Haller, have a financial interest in Caisson Biotech, LLC.

Literature Cited

- Abu Lila AS, Kiwada H, Ishida T. 2013. The accelerated blood clearance (ABC) phenomenon: Clinical challenge and approaches to manage. *J Control Release*, 172(1): 38–47.
- Acharya S, Sahoo SK. 2011. PLGA nanoparticles containing various anticancer agents and tumour delivery by EPR effect. *Advanced drug delivery reviews*, 63(3): 170–83.
- Aguiar J, Carpena P, Molina-Bolivar J, Carnero Ruiz C. 2003. On the determination of the critical micelle concentration by the pyrene 1:3 ratio method. *Journal of Colloid and Interface Science*, 258(1): 116–122.
- Albanese A, Tang PS, Chan WCW. 2012. The Effect of Nanoparticle Size, Shape, and Surface Chemistry on Biological Systems. *Annu Rev Biomed Eng*, 14(1): 1–16.
- Anders CK, Adamo B, Karginova O, Deal AM, Rawl S, Darr D, Schorzman A, et al. 2013. Pharmacokinetics and efficacy of PEGylated liposomal doxorubicin in an intracranial model of breast cancer. *PloS One*, 8(5): e61359.
- Armstrong, JK, Hempel G, Kolling S, Chan LS, Fisher T, Meiselman HJ, Garratty G. 2007. Antibody against poly(ethylene glycol) adversely affects PEG-asparaginase therapy in acute lymphoblastic leukemia patients. *Cancer*, 110(1): 103–111.
- Baggenstoss BA, Weigel PH. 2006. Size exclusion chromatography-multiangle laser light scattering analysis of hyaluronan size distributions made by membrane-bound hyaluronan synthase. 352(2): 243-251.
- Bathe M, Ruthedge GC, Grodzinsky AJ, Tidor B. 2005. A Coarse-Grained Molecular Model for Glycosaminoglycans: Application to Chondroitin, Chondroitin Sulfate, and Hyaluronic Acid. *Biophysical Journal*, 88(6): 3870–3887.

- Baumann A, Tuereck D, Dickmann L, Sims J. 2014. Pharmacokinetics, metabolism and distribution of PEGs and PEGylated proteins: quo vadis? *Drug Discovery Today*, 19(10):1623–1631.
- Bitter T, Muir HM. 1962. A modified uronic acid carbazole reaction. *Analytical Biochemistry*, 4(4): 330–334.
- Campbell KP, MacLennan DH, Jorgensen AO. 1983. Staining of the Ca²⁺-binding proteins, calsequestrin, calmodulin, troponin C, and S-100, with the cationic carbocyanine dye “Stains-all”. *Journal of Biological Chemistry*, 258(18):11267–11273.
- Chanan-Khan A, Szebeni J, Savay S, Liebes L, Rafique NM, Alving CR, Muggia FM. 2003. Complement activation following first exposure to pegylated liposomal doxorubicin (Doxil): possible role in hypersensitivity reactions. *Annals of Oncology*, 14(9):1430–7.
- Chen J-X, Liu W, Zhang M, Chen J-H. 2014. Heparosan based negatively charged nanocarrier for rapid intracellular drug delivery. *Int J Pharm*, 473(1–2): 493–500.
- Chen Y, Peng J, Han M, Omar M, Hu D, Ke X, Lu N. 2015. A low-molecular-weight heparin-coated doxorubicin-liposome for the prevention of melanoma metastasis. *Journal of Drug Targeting*, 23(4): 335–346.
- DeAngelis PL. 2015. Heparosan, a promising “naturally good” polymeric conjugating vehicle for delivery of injectable therapeutics. *Expert Opin Drug Deliv*, 12(3): 349–352.
- Fan W, Evans RM. 2015. Turning up the heat on membrane fluidity. *Cell*, 161(5): 962–3.

- Grobmeyer SR, Moudgil BM. 2010. *Cancer Nanotechnology: Methods and Protocols*. New York, NY: Humana Press: p3.
- Hamad I, Hunter AC, Szebeni J, Moghimi SM. 2008. Poly(ethylene glycol)s generate complement activation products in human serum through increased alternative pathway turnover and a MASP-2-dependent process. *Molecular Immunology*, 46(2): 225–232.
- Han N-K, Shin DH, Kim JS, Weon KY, Jang CY, Kim JS. 2016. Hyaluronan-conjugated liposomes encapsulating gemcitabine for breast cancer stem cells. *Int J Nanomedicine*, 11: 1413–25.
- Hotze EM, Le HM, Sieber JR, Bruxvoort C, McInerney MJ, Tweten RK. 2013. Identification and characterization of the first cholesterol-dependent cytolysins from Gram-negative bacteria. *Infection and immunity*, 81(1): 216–25.
- Ikegami-Kawai M, Takahashi T. 2002. Microanalysis of hyaluronan oligosaccharides by polyacrylamide gel electrophoresis and its application to assay of hyaluronidase activity. *Analytical Biochemistry*, 311(2): 157–165.
- Ishida T, Ichihara M, Wang XY, Yamamoto K, Kimura J, Majima E, Kiwada H. 2006. Injection of PEGylated liposomes in rats elicits PEG-specific IgM, which is responsible for rapid elimination of a second dose of PEGylated liposomes. *J Control Release*, 112(1): 15–25.
- Ishida T, Kiwada H. 2008. Accelerated blood clearance (ABC) phenomenon upon repeated injection of PEGylated liposomes. *Int J Pharm*, 354(1–2): 56–62.
- Ivens IA, Achanzar W, Baumann A, Brandli-Baiocco A, Cavagnaro J, Dempster M, Depelchin BO, et al. 2015. PEGylated Biopharmaceuticals: Current Experience and

Considerations for Nonclinical Development. *Toxicologic Pathology*, 43(7): 959–983.

Jing W, Roberts JW, Green DE, Almond A, DeAngelis PL. 2017. Synthesis and Characterization of Heparosan-Granulocyte-Colony Stimulating Factor Conjugates: a natural sugar-based drug delivery system to treat neutropenia. Manuscript submitted for publication.

Lee HG, Cowman MK. 1994. An Agarose Gel Electrophoretic Method for Analysis of Hyaluronan Molecular Weight Distribution. *Analytical Biochemistry*, 219(2): 278–287.

Li L, Zhang F, Zaia J, Linhardt RJ. 2012. Top-down approach for the direct characterization of low molecular weight heparins using LC-FT-MS. *Analytical chemistry*, 84(20): 8822–9.

Liu Y, Mihsi V, Kubiak R, Rebecchi M, Bruzik K. 2007. Phosphorothiolate Analogues of Phosphatidylinositols as Assay Substrates for Phospholipase C. *ChemBioChem*, 8(12): 1430–1439.

Lubich C, Allacher P, de la Rosa M, Bauer A, Prenninger T, Horling FM, Siekmann J, et al. 2016. The Mystery of Antibodies Against Polyethylene Glycol (PEG) - What do we Know? *Pharmaceut Res*, 33(9): 2239–2249.

Mamidi RNVS, Weng S, Stellar S, Wang C, Yu N, Huang T, Tonelli AP, et al. 2010. Pharmacokinetics, efficacy and toxicity of different pegylated liposomal doxorubicin formulations in preclinical models: Is a conventional bioequivalence approach sufficient to ensure therapeutic equivalence of pegylated liposomal doxorubicin products? *Cancer Chemother Pharmacol*, 66(6):1173–1184.

Nag OK, Yadav VR, Croft B, Hedrick A, Awasthi V. 2015. Liposomes Modified with Superhydrophilic Polymer Linked to a Nonphospholipid Anchor Exhibit Reduced Complement Activation and Enhanced Circulation. *J Pharm Sci*, 104(1): 114–123.

Nag OK, Yadav VR, Hedrick A, Awasthi V. 2013. Post-modification of preformed liposomes with novel non-phospholipid poly(ethylene glycol)-conjugated hexadecylcarbamoylemethyl hexadecanoic acid for enhanced circulation persistence in vivo. *Int J Pharm*, 446(1–2): 119–29.

"PEGylated Doxosome." 2014. Retrieved from www.doxosome.com/pegylated-doxosome-2/ [Accessed March 9, 2017].

National Center for Health Statistics, 2016. Health, United States, 2015: With Special Feature on Racial and Ethnic Health Disparities. *Health, United States, 2015: With Special Feature on Racial and Ethnic Health Disparities*, p.107. Available at: <http://www.ncbi.nlm.nih.gov/pubmed/27308685>.

Ortega A, Amorós D, and de la Torre JG. 2011. Prediction of hydrodynamic and other solution properties of rigid proteins from atomic- and residue- level models. *Biophysical Journal*, 101(4): 892-898.

Pöschel KA, Bucha E, Esslinger H-U, Nortersheuser P, Jansa U, Schindler S, Nowak G, et. al. 2000. Pharmacodynamics and pharmacokinetics of polyethylene glycol-hirudin in patients with chronic renal failure. *Kidney Intl*, 58(6): 2478–2484.

Rafiyath SM, Rasul M, Lee B, Wei G, Lamba G, Liu D. 2012. Comparison of safety and toxicity of liposomal doxorubicin vs. conventional anthracyclines: a meta-analysis. *Exp Hematol Oncol*, 1(1): 10.

Rosenthal K. 2002. Rodent Reference Ranges. Available at:

<http://cal.vet.upenn.edu/projects/ssclinic/refdesk/rodentrr.htm> [Accessed January 5, 2017].

Sathyamoorthy N, Dhanaraju MD. 2016. Shielding Therapeutic Drug Carriers from the Mononuclear Phagocyte System: A Review. *Crit Rev Ther Drug Carrier*, 33(6), pp.489–567.

Sattelle BM, Shakeri J, Almond AA. 2013. Does microsecond sugar ring flexing encode 3D-shape and bioactivity in the heparanome? *Biomacromolecules*, 14(4): 1149–59.

Sherman M, Seth A, Delp S. 2011. Simbody: multibody dynamics in biomedical research. *Procedia IUTAM*, 2: 241–261.

Sismey-Ragatz AE, Green DE, Otto NJ, Rejzek M, Field RA, DeAngelis PL. 2007. Chemoenzymatic synthesis with distinct *Pasteurella* heparosan synthases: monodisperse polymers and unnatural structures. *J Biol Chem*, 282(39): 28321–7.

Uster PS, Allen TM, Daniel BE, Mendez CJ, Newman MS, Zhu GZ. 1996. Insertion of poly(ethylene glycol) derivatized phospholipid into pre-formed liposomes results in prolonged in vivo circulation time. *FEBS Letters*, 386(2–3): 243–246.

Waterhouse DN, Tardi PG, Mayer LD, Bally MB. 2001. A Comparison of Liposomal Formulations of Doxorubicin with Drug Administered in Free Form. *Drug Safety*, 24(12): 903–920.

Yang Q, Ma Y, Zhao Y, She Z, Wang L, Li J, Wang C, et. al. 2013. Accelerated drug release and clearance of PEGylated epirubicin liposomes following repeated injections: a new challenge for sequential low-dose chemotherapy. *Int J of Nanomedicine*, 8(1): 1257–68.

Yokomichi N, Nagasawa T, Coler-Reilly A, Suzuki H, Kubota Y, Yochioka R, Tozawa A, et al. 2013. Pathogenesis of Hand-Foot Syndrome induced by PEG-modified liposomal Doxorubicin. *Human cell*, 26(1): 8–18.

Zhou B, Weigel JA, Fauss L, Weigel PH. 2000. Identification of the hyaluronan receptor for endocytosis (HARE). *J Biol Chem*, 275(48): 37733–41.

Table

Table I. Comparison of Liposome Hydrodynamic Diameters by Dynamic Light Scattering (DLS) Experimental Measurement and by Molecular Simulations

The diameter of dox-liposomes coated with various heparosan chain sizes by post-insertional modification with 0.5 mol% of various 7- to 20-kDa HEP-lipid derivatives were both predicted *in silico* and measured experimentally ('Uncoated' = starting drug-loaded liposomes). The simulation and DLS data are in general agreement for smaller HEP chains, but more divergence is seen for the largest HEP polymer.

	<u>Diameter (nm)</u>		Method Differential (nm) ^a
	Simulation	DLS	
Uncoated	118 ^b	120	
7-kDa	137	137	
<u>Δ^c</u>	19	17	2
12.5-kDa	150	147	
<u>Δ</u>	□32	27	5
13.3-kDa	151	149	
<u>Δ</u>	33	29	4
20-kDa	173	159	
<u>Δ</u>	55	39	16

^a "Method Differential" represents the divergence between the DLS and the simulation diameters.

^b Simulation uncoated diameter was manually entered, not measured.

^c Δ = coated diameter minus uncoated diameter.

Figure Legends

Figure 1: Synthetic Scheme and Gel Characterization of HEP-Lipid Anchors

A) A schematic representing the heparosan repeating unit, and the HEP-NH₂ parental polymer and the HEP-lipid derivative syntheses. Briefly, the HEP backbone synthesis is primed with an amine-containing HEP trisaccharide acceptor (*white rectangle*) that is extended with donor UDP-sugars via PmHS1 to synthesize quasi-monodisperse HEP-NH₂ polysaccharide (*black/white rectangle*). The HEP-NH₂ is then reacted with different activated reagents to create HEP-lipid derivatives with either 1 or 2 palmitoyl (C16) tails (*note*: only the first reducing-end GlcA sugar of the HEP chain is shown here). B) Different HEP-lipid derivatives (7-kDa, 12.5-kDa, or 20-kDa HEP-Palm; 13.3-kDa HEP-DiPalm; 2 µg/lane; “-P” = *Palm*; “-DiP” = *DiPalm*), alongside their HEP-NH₂ parent (“-NH₂” = *amine*), were run on an 8% PAGE gel and stained with Alcian Blue. Note that the 13.3-kDa HEP-DiPalm forms aggregates (micelles), evidenced by staining in the well (lane 6).

Figure 2: Dynamic Light Scattering Analysis (DLS) of HEP-Lipid Coated Dox-liposomes and Susceptibility to GAG Degradation Enzymes

A) Various sizes of HEP-Palm monomers were incubated with dox-liposomes to assess the effect of the HEP coating on hydrodynamic diameter as measured via DLS. There was a clear chain size-dependent increase in diameter ($p < 0.0001$).

B) 12.5 kDa HEP-Palm or 13.3-kDa HEP-DiPalm coated liposomes (1 mol%) were measured by DLS before (*black*) and after incubation with heparinase III (cuts heparosan; *grey*) or hyaluronidase (HAase; *striped*). HAase did not modify HEP-coated

dox-liposome diameters as expected, but HEP lyase reduced the dox-liposomes to their original, uncoated size (*white*; note: two different uncoated dox-liposome preparations were used in these tests thus different 'un-coated' diameters). Dox-liposome diameter can be modified by using HEP-lipids with varying chain lengths (statistics: TwoWay ANOVA with Uncorrected Fischer's Least Significant Differences).

Figure 3: HEP-Palm and HEP-DiPalm Dox-liposome Coating Optimization as Characterized by DLS

The effect of HEP-lipid concentration and incubation temperature on dox-liposome size was measured. Panel A, 12.5-kDa HEP-Palm (0.5, *black*, or 1 mol% *white*) or Panel B, 13.3-kDa HEP-DiPalm (0.5, *black*, or 2 mol%, *white*). The HEP-lipids were incubated with dox-liposomes for 1 hour at 22°, 37°, or 50°C and assessed by DLS measurement. Higher HEP-Palm concentration did not increase dox-liposome diameter at any temperature. Elevated temperatures, however, significantly reduced the HEP-Palm coated dox-liposome diameter ($p < 0.001$) at both concentrations, suggesting impaired HEP-Palm association. Both temperature and concentration effectively increased the diameter of dox-liposomes incubated with HEP-DiPalm ($p < 0.01$ for temperature, $p < 0.0001$ for concentration). Dox-liposomes incubated with 0.5 mol% HEP-DiPalm at 50°C were significantly larger than those incubated at 22° and 37°C, suggesting improved HEP-DiPalm association at higher temperatures ($p < 0.05$, $p < 0.005$, respectively; statistics: TwoWay ANOVA with Uncorrected Fischer's Least Significant Differences).

Figure 4: Representation of HEP-Liposome Assembly

Models of HEP-coated liposome assemblies with 13.3-kDa (*top*) and 7-kDa (*bottom*) HEP-lipid, based on typical molecular configurations from equilibrated coarse-grained simulations. The liposome and sugars are represented graphically by equivalent spheres (roughly to scale), and part of the liposome has been cut-away for viewing purposes. Potential interaction proteins are depicted (human serum albumin, *HSA*; immunoglobulins *IgG* or *IgM*; *middle*), drawn to exact scale using coordinates from the Protein Data Bank. Less surface area is available for direct protein binding to liposomes coated with 0.5 mol% 13.3-kDa HEP-lipid compared to 0.5 mol% 7-kDa HEP-lipid, suggesting increased liposomal protection from clearance by the immune system. The image was rendered using POV-Ray software.

Figure 5: HEP-DiPalm Stability Assessment with [³H]Sugar Probe and Size Exclusion Chromatography

A liposome preparation with radioactive HEP-DiPalm probe was split into three equal portions. One portion, representing the starting material, was immediately re-analyzed by SEC (“initial,” *solid line*). The two other portions were challenged at 37°C with either PBS (*dashed line*) or human plasma (*dotted line*). The next day, SEC was used to quantify the amount of dox-liposome-associated counts retained in these two challenged samples. The radioactivity in the liposomal fraction (the void volume, shown here) of each run was compared; roughly 80% retention of [³H]HEP-DiPalm with the dox-liposome was observed in the plasma sample, indicating that the HEP-DiPalm coating was relatively stable on the liposome under conditions mimicking the

composition of the bloodstream.

Figure 6: DLS Size Analysis of Efficacy Study Dox-liposomes

For animal efficacy studies, uncoated dox-liposomes were incubated with either 12.5-kDa HEP-Palm or 13.3-kDa HEP-DiPalm at 0.5 mol%. Prior to injection, a sample from each treatment group was removed for measurement by DLS. HEP-Palm and HEP-DiPalm significantly increased the uncoated dox-liposome size from 129 nm to approximately 158 nm and 159 nm, respectively (means estimated from all batches; OneWay ANOVA, $p < 0.0001$). HEP-Palm and HEP-DiPalm were not significantly (“n.s.”) different from each other (Tukey’s Multiple Comparisons Test, $p = 0.87$). PEGylated dox-liposomes were ~123 nm and derived from an independent formulation (PEG-lipid was not added by post-insertional modification).

Figure 7: Assessment of Drug Efficacy in Rats by Tumor Volume, Mass, and Necrosis

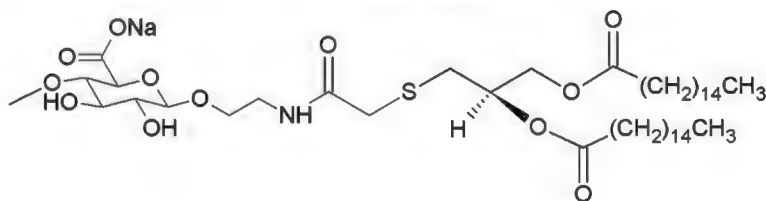
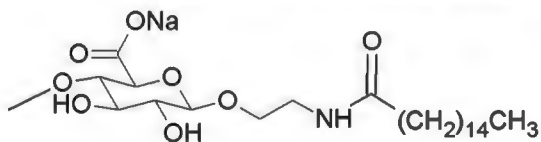
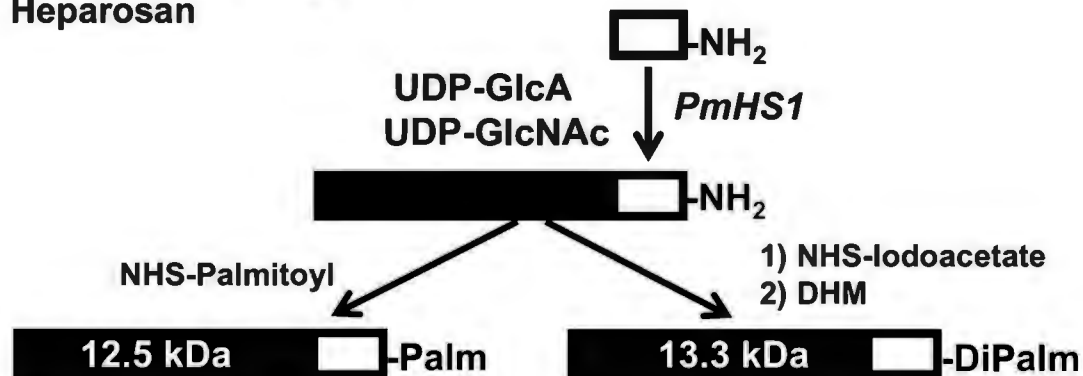
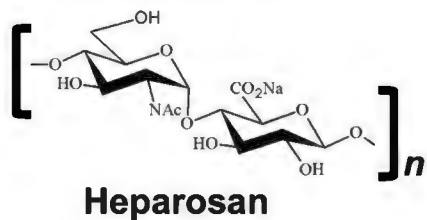
The MDA-MD-231 human breast cancer xenograft mouse model was used to assess the relative efficacy of the various dox-liposome formulations. A) Tumor volume in living mice was measured via TumorImager every five days. Both HEP-DiPalm (*white squares*) and PEGylated (*white circles*) dox-liposomes significantly reduced tumor volume compared to uncoated (*black triangles*) and HEP-Palm (*white triangles*) dox-liposomes at day 34 ($p < 0.005$, $p < 0.05$ respectively), but were not significantly (“n.s.”) different from each other ($p = 0.3429$). B) The observed tumor weight post-mortem of the groups followed the same pattern as volume. Both HEP-DiPalm and PEG reduced

tumor mass compared to uncoated dox-liposomes ($p < 0.05$ for both), but were not significantly different from each other ($p = 0.4656$). C) Tumor necrosis was evaluated by microscopy with hematoxylin and eosin staining. Necrosis was significantly higher in mice treated with HEP-DiPalm dox-liposomes ($p < 0.01$). Overall, the HEP-DiPalm-coated drug performed similarly to FDA-approved PEG-based drug and may lend added potency. One-way ANOVA, Uncorrected Fishers LSD used for all statistics.

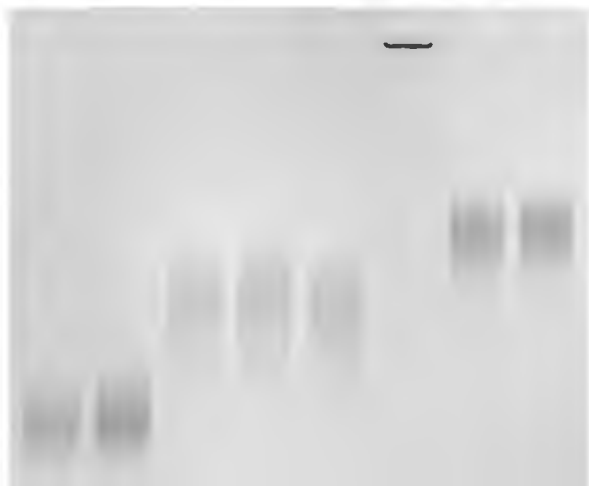
Figure 8: Immunological Challenge in Rats with HEP-DiPalm and ELISA

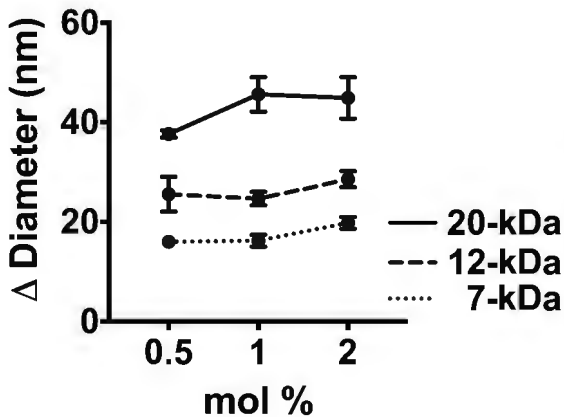
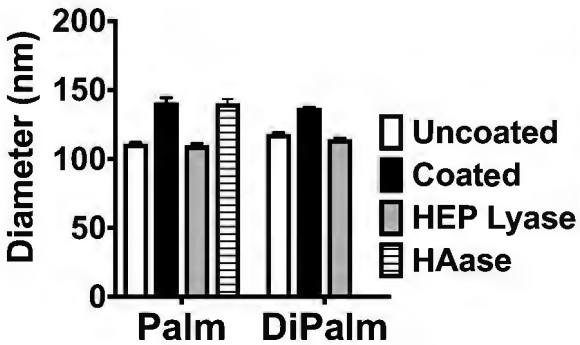
Assessment.

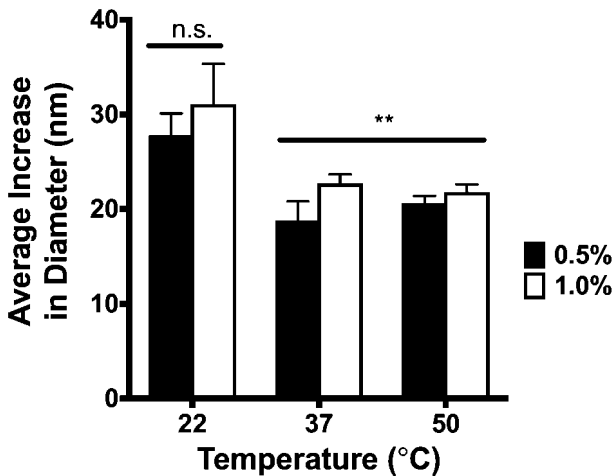
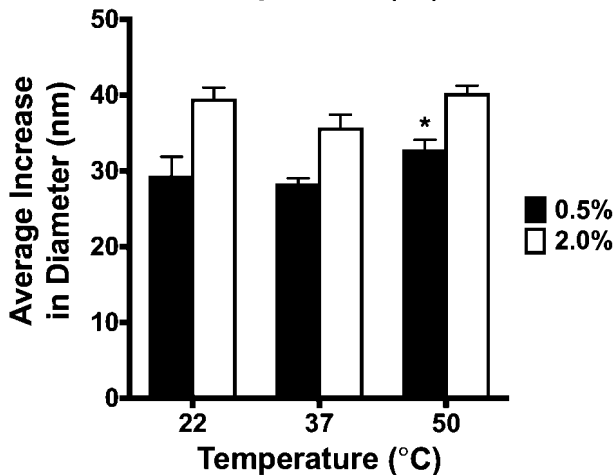
A set of three rats (#1, 2, 3) was boosted with a series of HEP-conjugates in a long-term study (see **Supplementary Fig. 4**) then tested for the induction of an IgM or IgG response by ELISA (representative set of assays with averaged triplicate wells with standard deviation is presented). Overall, the signal from sera of rats before and after injection with HEP-DiPalm micelles (pre-lipid, *white*; post-lipid, *black*) tested in the control wells coated with bovine serum albumin (*BSA*) was equivalent to the wells coated with HEP-BSA (*HEP*) or HEP-DiPalm (*DiPalm*) indicating that heparosan is not significantly immunogenic, therefore, should be useful in multi-dose or long-term therapeutics.

A.**B.**

Mass (kDa)	6.7	6.7	12.5	12.5	13.3	13.3	20	20
Termini	-NH ₂	-P	-NH ₂	-P	-NH ₂	-DiP	-NH ₂	-P



A.**B.**

A.**B.**

13-kDa HEP



HSA 

IgG 

IgM 

7-kDa HEP

